OPEN ACCESS
Journal of Innovative Optical Health Sciences
Vol. 14, No. 2 (2021) 2150005 (9 pages)

DOI: 10.1142/S179354582150005X

World Scientific
www.worldscientific.com

Determination of diffusion coefficient by image-based fluorescence recovery after photobleaching and single particle tracking system implemented in a single platform

Donghee Lee
Department of Genetics, Cell Biology and Anatomy
University of Nebraska Medical Center, Omaha, NE 68198, USA

Jeonghoon Lee*
School of Mechanical Engineering
KOREATECH, Cheonan 31253, Republic of Korea
jlee@koreatech.ac.kr

Jung Kyung Kim*
School of Mechanical Engineering and Department of
Integrative Biomedical Science and Engineering
Graduate School, Kookmin University
Seoul 02707, Republic of Korea
jkkim@kookmin.ac.kr

Received 16 July 2020
Accepted 25 November 2020
Published 30 December 2020

Fluorescence recovery after photobleaching (FRAP) and single particle tracking (SPT) techniques determine the diffusion coefficient from average diffusive motion of high-concentration molecules and from trajectories of low-concentration single molecules, respectively. Lateral diffusion coefficients measured by FRAP and SPT techniques for the same biomolecule on cell membrane have exhibited inconsistent values across laboratories and platforms with larger diffusion coefficient determined by FRAP, but the sources of the inconsistency have not been investigated thoroughly. Here, we designed an image-based FRAP-SPT system and made a direct comparison between FRAP and SPT for diffusion coefficient of submicron particles with known theoretical values derived from Stokes–Einstein equation in aqueous solution. The combined *i*FRAP-SPT technique allowed us to measure the diffusion coefficient of the same fluorescent particle by utilizing both techniques in a single platform and to scrutinize inherent errors and artifacts of FRAP. Our results reveal that diffusion coefficient overestimated by FRAP is caused by inaccurate estimation of the bleaching spot size and can be corrected by simple image analysis. Our *i*FRAP-SPT technique can be potentially used for not only cellular membrane dynamics but

*Corresponding authors.

also for quantitative analysis of the spatiotemporal distribution of the solutes in small scale analytical devices.

Keywords: Diffusion coefficient; fluorescence recovery after photobleaching (FRAP); single particle tracking (SPT).

1. Introduction

Fluorescence recovery after photobleaching (FRAP) and single particle tracking (SPT) have been used to estimate the diffusion coefficients of macromolecules in biological media because diffusion process is a key mechanism for biomolecular transport in micro-environment such as scaffolds and membranes. In addition, quantitative measurement of diffusion of solutes is crucial in drug delivery system and cell morphogenesis. In the FRAP system, a micron-sized region full of fluorophores is instantaneously bleached by a high-intensity laser irradiation. Subsequently, fluorescence is recovered by the diffusion of both bleached and unbleached molecules and diffusion coefficient is determined by analysis of the fluorescence recovery curve. FRAP had been originally devised by Axelrod *et al.*[1] and has been improved by a number of researchers.[2–4] As opposed to FRAP, SPT traces the trajectory of each molecule conjugated with nanoparticles and reveals the structure of cell membrane as well as the dynamic behavior of the molecule. SPT also has been studied for many years and applied to various areas, such as measurement of diffusion coefficient of quantum dot-labeled protein[5] and membrane receptors conjugated with gold nanoparticles.[6]

Despite many researches, diffusion coefficients determined by FRAP (D_{FRAP}) were found to be inconsistent with SPT measurement (D_{SPT}). Saxton and Jacobson[7] reported that D_{FRAP} was $4-7$ times higher than the apparent D_{SPT} for the mobile fraction of lipids and GPI (glycosylphosphatidylinositol)-linked proteins at the membrane of cells such as fibroblast and myoblast. Guo *et al.*[8] measured lateral lipid diffusion in supported lipid bilayers and giant unilamellar vesicles by SPT and FRAP on the same samples using different instruments. They found that D_{FRAP} was biased to larger or smaller values compared with D_{SPT} depending on the length scales and temporal resolution.[8] The disagreement of the diffusion coefficients is caused by interlaboratory or intersystem variations of several factors, including the condition of sample, labeling marker, detecting platform and microenvironment.[7–9] Nevertheless, the errors in diffusion coefficients measured by FRAP and SPT have not been quantitatively analyzed at the same platform. Stimulated by this, we developed a novel diffusion measurement technique, image-based FRAP-SPT (*i*FRAP-SPT), to determine D_{FRAP} and D_{SPT} from both methods in a single platform, respectively. In this study, a direct comparison between FRAP and SPT was made for diffusion of submicron particles in aqueous solution with a newly designed *i*FRAP-SPT system, which could address the sources of inherent errors in both techniques.

2. Experimental Methods

2.1. *Sample preparation*

We prepared suspensions of 210 nm (FC02F, Bangs Laboratories; $\lambda_{\mathrm{ex,peak}} = 480\,\mathrm{nm}/\lambda_{\mathrm{em,peak}} = 520\,\mathrm{nm}$) and 500 nm (Fluosphere F8813, Invitrogen; 505 nm/515 nm) fluorescent particles in distilled water to compare D_{FRAP} with D_{SPT}. Concentrations of 210 nm and 500 nm particles were 2 mg/mL and 4 mg/mL, respectively. We also prepared 70 kDa fluorescein dextran (D1823, Invitrogen; 494 nm/521 nm) solution with concentration of 20 mg/mL to estimate the axial bleaching profile in 3D FRAP measurement. For further testing of the *i*FRAP-SPT system, we also prepared specially designed 1 μm fluorescent particle (T8880, Invitrogen; 488 nm/560 nm) suspension at the concentration of 2.5 mg/mL.

As shown in Fig. 1(a), a sample chamber was prepared by attaching two coverslips (18 mm × 18 mm) spaced by 18 mm onto a glass slide (25 mm × 75 mm) and a coverslip (18 mm × 50 mm) is placed on top of the attached coverslips to make a 170 μm gap between the bottom slide and the upper coverslip. We filled the space ($\sim 55\,\mu$L) with the particle suspension and the edges of the slide were sealed with colorless nail-polish to avoid drying. Images were acquired

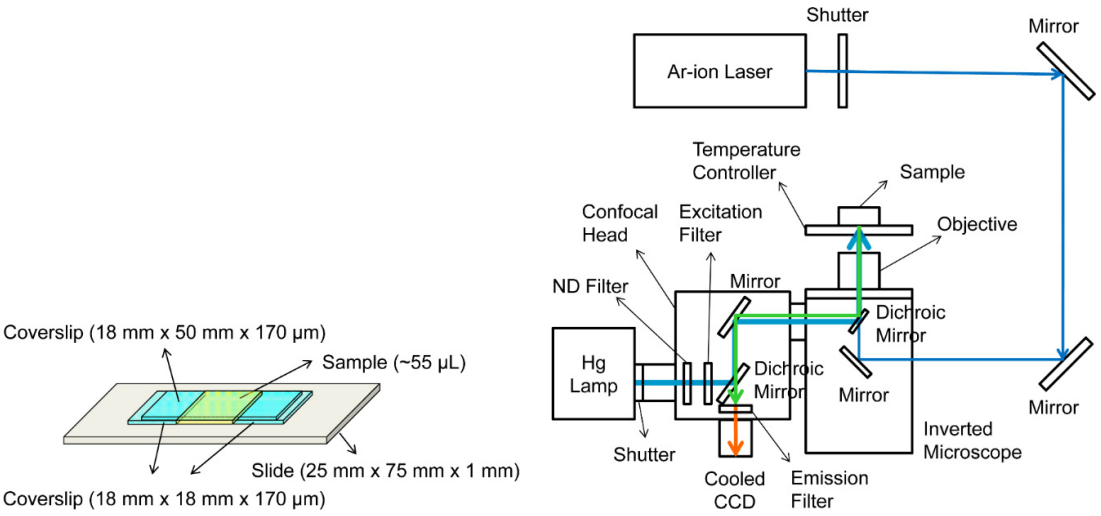

Fig. 1. (a) Schematic of sample chamber made of a slide and coverslips. (b) Configuration of *i*FRAP-SPT system.

through the slide glass placed at the bottom of the sample chamber. The temperature of the samples was maintained at 25°C using a heating plate (HP-R-10, Live Cell Instrument) during the measurement to minimize the effect of temperature on the determination of diffusion coefficients.

2.2. *Instrumentation*

Figure 1(b) is the schematic of our *i*FRAP-SPT configuration. In the present system, careful attention should be paid to the alignment of the excitation laser beam which was solely used for photobleaching the fluorescent sample. A 488 nm Ar-ion laser beam (35 LAP 431, Melles Griot) was aligned using two pinholes and two mirrors to be focused near the center of the sample. We used two pinholes to confirm that the Ar-ion laser was propagated parallel to the optical bread board where optical components were installed. We adjusted two mirrors to control the direction of the beam toward an inverted microscope. We made a fine adjustment of the mirrors again, which enabled the laser beam to be aligned on the sample.

In the FRAP experiments, we bleached the sample for approximately 250 ms with the laser beam at the output power of 23 mW through a 40 × /0.75 NA objective (UPlanFL N, Olympus), and the bleaching time was controlled by the shutter located in front of the laser. To illuminate the fluorescent particle suspension, we used a mercury lamp with a neutral density filter; thus, we could monitor the fluorescence recovery at 0.09 mW. The fluorescence images were acquired by a CCD camera (Sensicam, PCO) at 4 frames per second after photobleaching the sample at an inverted fluorescence microscope (IX71, Olympus). We used a software (AQM6, Kinetic Imaging) to control the laser shutter in synchronous with the camera.

3. Data Analysis

During FRAP experiments, we obtained the time-series images of the samples as well as the fluorescence recovery curves as shown in Fig. 2. Photobleached spots are clearly observed at time 0 and the bleached spot is recovered thereafter, as shown in Fig. 2(a). ImageJ software (http://rsb.info.nih.gov/ij/) was used to analyze the time series images procured from FRAP and SPT. We obtained gray level pixel values in the bleached area for the FRAP analysis and normalized them by plotting the fractional fluorescence recovery curve given as follows:

$$f(t) = \frac{F(t) - F(0)}{F(\infty) - F(0)}, \tag{1}$$

where $F(t)$ is the fluorescence intensity at indicated time, $F(0)$ represents the fluorescence intensity immediately after photobleaching and $F(\infty)$ denotes the fluorescence intensity at the moment when the recovery is complete. Lateral diffusion coefficient, D_{FRAP}, can be determined by fitting $f(t)$ to the equations below for the bleaching

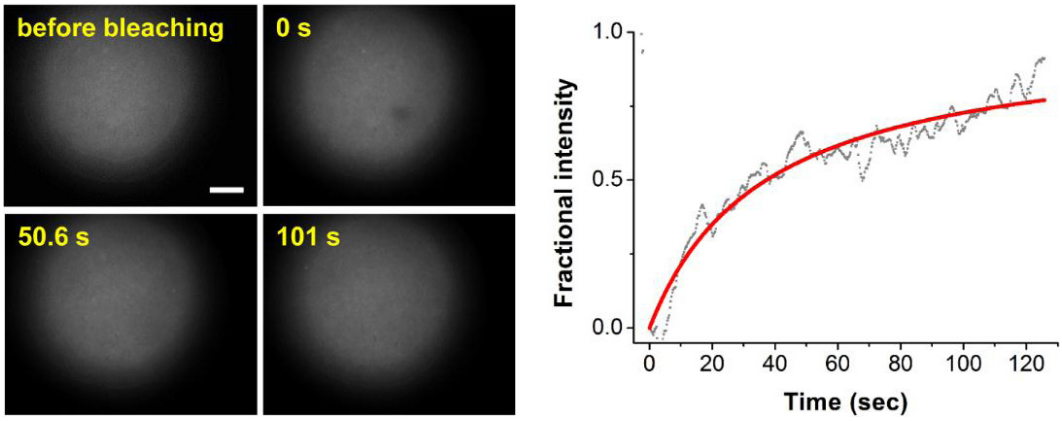

(a) (b)

Fig. 2. (a) FRAP images of fluorescent particles ($d = 210$ nm). Photobleached spot recovers by particle diffusion with increasing time. Scale bar = 50 μm. (b) Corresponding fluorescence recovery curves.

intensity with a uniform circular disk profile of radius w_0:

$$f(t) = \exp\left(-\frac{2\tau_D}{t}\right)\left[I_0\left(\frac{2\tau_D}{t}\right) + I_1\left(\frac{2\tau_D}{t}\right)\right], \quad (2)$$

where I_0 and I_1 are modified Bessel functions and $\tau_D = w_0^2/4D$, and with a Gaussian profile[1]

$$f(t) = \frac{F(t)/F(\infty) - F(0)/F(\infty)}{1 - F(0)/F(\infty)},$$

$$F(t)/F(\infty) = \sum_{n=0}^{\infty} \frac{(-K)^n}{n!} \frac{1}{1 + n + 2nt/\tau_D}, \quad (3)$$

where K is a bleaching factor. $F(0)/F(\infty) = \exp(-K)$ for the uniform circular disk and $F(0)/F(\infty) = K^{-1}[1 - \exp(-K)]$ for the Gaussian profile. Equations (2) and (3) assume 2D free diffusion in a bleached region without recovery from above and below the focal plane.

We also fitted the data using an analytical solution given for the 3D photobleaching measurement of isotropic diffusion with same 3D Gaussian profile for illumination and detection[10]: $I(x, y, z) = I_0 \exp[-(x^2 + y^2)/w_0^2 - z^2/w_{z0}^2]$, where I_0 is the maximum illumination intensity and w_0 and w_{z0} are the beam waists in the radial and axial directions, respectively. The fluorescence recovery for 3D isotropic free diffusion is given by

$$F(t)/F(\infty) = \sum_{n=0}^{\infty} \frac{(-K)^n}{n!} \times \frac{1}{(1 + n + 2nt/\tau_D) \times \sqrt{(1 + n + 2nt/\alpha\tau_D)}}, \quad (4)$$

where $\alpha = w_{z0}^2/w_0^2$ which defines axial bleaching profile with a given w_0. The bleaching factor, K, was chosen to produce an approximately 50% reduction in fluorescence immediately following bleaching. $K = 0.69$, 1.59, and 2.5 for uniform circular disk profile, 2D Gaussian profile, and 3D Gaussian profile, respectively.

Figure 2(b) shows $f(t)$ measured for diffusion of 210 nm particles and a fitted curve with Eq. (3). We determined D_{FRAP} of the particles in water using Eqs. (2)–(4) with $w_0 = 21.1$ μm measured by laser beam profiler (SP620U, Ophir Optronics Solutions) and $\alpha = 9.59$ obtained by setting it as a free parameter in analysis of $f(t)$ for diffusion of dextran. The uncertainty on α is ± 3.72 with 95% confidence bounds.

Figure 3(a) shows the representative trajectory of a 210 nm particle diffused in water. STP analysis was conducted according to the method reported by Haggie *et al.*[5] We calculated the mean square displacement (MSD) from the trajectory of each particle traced by ImageJ manual tracking plugin. For the randomly diffusing particles, MSD is defined as follows:

$$\mathrm{MSD} = \langle r^2(n\delta t)\rangle = \frac{1}{N-n} \sum_{j=0}^{N-n-1} \times \{[x(j\delta t + n\delta t) - x(j\delta t)]^2 + [y(j\delta t + n\delta t) - y(j\delta t)]^2\} \quad (n = 0, 1, 2, \ldots, N-1), \quad (5)$$

where δt is the time step, $(x(j\delta t), y(j\delta t))$ is the particle position at time $t = j\delta t$ and N is the total

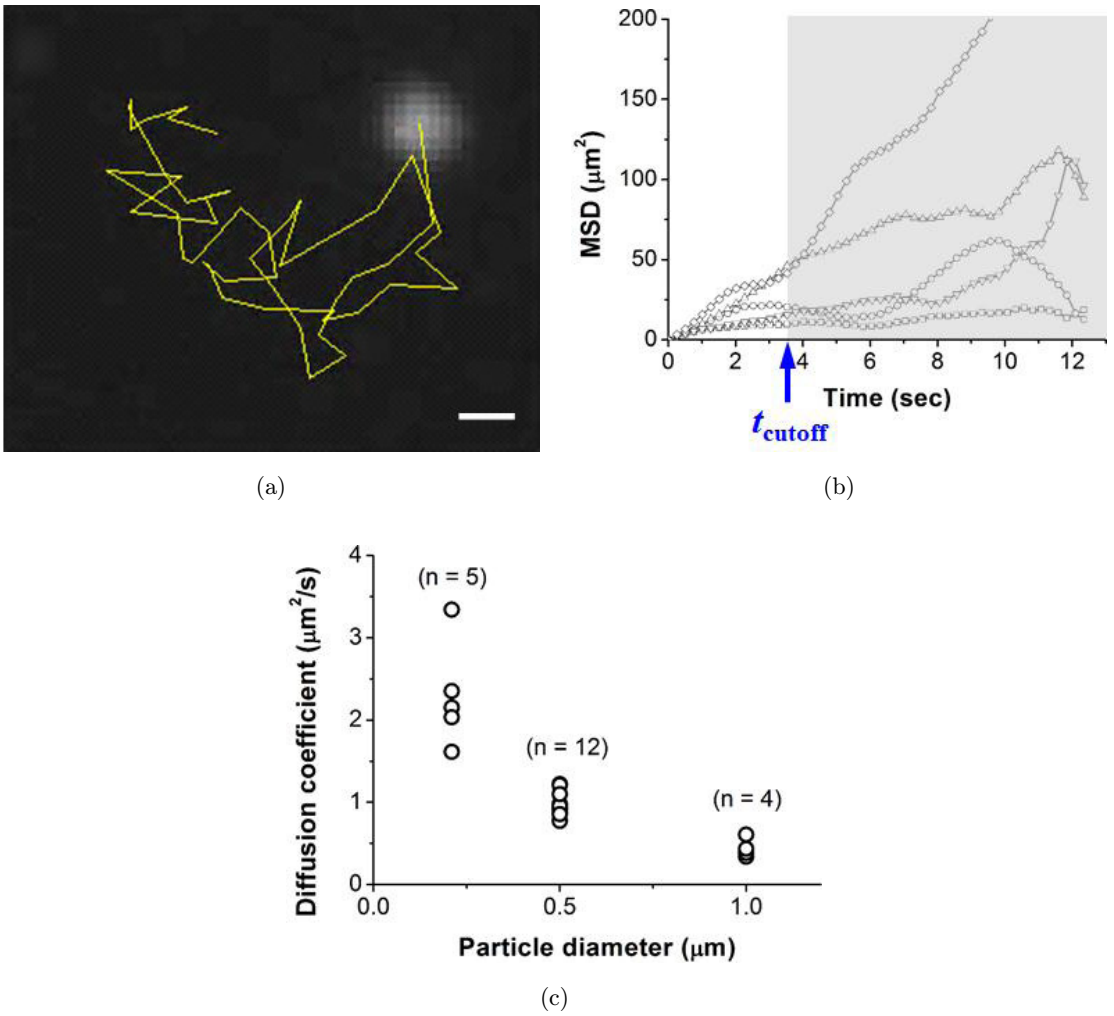

Fig. 3. (a) SPT trajectory of 210 nm particle. Scale bar = 2 μm. (b) MSD versus time plot. (c) Microscopic diffusion coefficients for particles with different diameters (d = 210 nm, 500 nm and 1 μm). n = number of particle trajectories.

number of images acquired for an individual particle. The centroid of the particle image was used to generate a particle trajectory and those particles moving out of focal plane were not considered in SPT analysis to determine lateral D_{SPT}.

The MSD curve obtained by Eq. (5) shows fluctuations for large time intervals, as shown in Fig. 3 (b), because the number of data points is not sufficient to give a small standard deviation. Thus, we need to determine a cutoff time (t_{cutoff}) for each MSD curve. We used $t_{\mathrm{cutoff}} = N/4$ and confirmed the validity from the analysis of particle trajectories generated by Monte Carlo simulation. Least squares fitting was conducted by using the first three points on each MSD versus time plot to determine the microscopic diffusion coefficient, $D_{0-2} = \mathrm{MSD}_{0-2}/4(2\delta t)$. D_{SPT} of the particles were computed by taking averages of D_{0-2} values plotted in Fig. 3(c). D_{0-2} values measured for 1 μm particle are added as reference.

4. Results and Discussion

We used different-sized submicron particles as samples for this study because we could compare diffusion coefficient of the particles measured by both FRAP and SPT with those obtained by Stokes–Einstein equation given as follows:

$$D_{\mathrm{SE}} = \frac{k_B T}{3\pi\eta d}, \tag{6}$$

where k_B is Boltzmann's constant (1.38×10^{-23} J/K), η is the viscosity of water at 298 K (0.91 cP), T is the absolute temperature of water (298 K), and d is the particle diameter (210 nm or 500 nm). For dilute particle suspensions, the ratio of viscosity

Table 1. Diffusion coefficients (D) determined by FRAP, SPT and Stokes–Einstein equation.

	FRAP[a]			
Sample / D*(μm^2/s)	$w_0 = 21.1\,\mu$m	w_0 (corrected) $= 18.0\,\mu$m	SPT[b]	Stokes–Einstein equation
Fluorescent particle ($d = 210$ nm)	2.67 ± 0.06 (2D uniform disk) 3.13 ± 0.07 (2D Gaussian) 3.23 ± 0.07 (3D Gaussian, $\alpha = 9.59$)	1.95 ± 0.04 (2D uniform disk) 2.28 ± 0.05 (2D Gaussian) 2.35 ± 0.05 (3D Gaussian, $\alpha = 9.59$)	2.30 ± 0.31 ($n = 5$)	2.28
Fluorescent particle ($d = 500$ nm)	1.23 ± 0.04 (2D uniform disk) 1.49 ± 0.05 (2D Gaussian) 1.52 ± 0.06 (3D Gaussian, $\alpha = 9.59$)	0.89 ± 0.03 (2D uniform disk) 1.09 ± 0.04 (2D Gaussian) 1.11 ± 0.04 (3D Gaussian, $\alpha = 9.59$)	0.96 ± 0.15 ($n = 12$)	0.96

Note: *All values are reported as mean ± standard deviation.
[a]The standard deviations are obtained from curve fitting.
[b]The standard deviations are obtained from repeated experiments.

with monosized particles (η) divided by the viscosity of the pure fluid (η_f) can be described by

$$\frac{\eta}{\eta_f} = 1 + 2.5\phi + 6.2\phi^2, \tag{7}$$

where ϕ is the particle volume concentration.[11] If we assume $\phi = 1\%$, which is 2.5–100 times higher than what we used, then $\eta/\eta_f = 1.0256$, implying that even 1% particle suspension does not affect the viscosity of the solution nor diffusion coefficient of the particle significantly.

Table 1 shows the comparison between D_{FRAP}, D_{SPT}, and D_{SE}. There is a fairly good agreement between D_{SPT} and D_{SE} ($2.30\,\mu$m^2/s versus $2.28\,\mu$m^2/s for 210 nm and $0.96\,\mu$m^2/s versus $0.96\,\mu$m^2/s for 500 nm particles). D_{FRAP} exhibits the largest values regardless of the fitting equation (2.67–3.23 μm^2/s for 210 nm and 1.23–1.52 μm^2/s for 500 nm particles). The standard deviations are obtained from the curve fitting for FRAP and from repeated experiments for SPT.

The $1/e^2$ radii in the lateral and axial dimensions of the bleaching volume were $w_0 = 18.0\,\mu$m and $w_{z0} = 55.7\,\mu$m, respectively. The axial bleaching dimension ($2w_{z0}$) is less than the thickness $= 170\,\mu$m of the sample chamber, which ensures that isotropic free diffusion occurs in the three-dimensional (3D) space at our experimental setup. In the FRAP analysis of isotropic free diffusion, diffusion coefficient is scaled with w_0^2/τ_D where τ_D can be determined by fitting measured $f(t)$ to Eqs. (2)–(4). As τ_D values computed from our Monte Carlo simulation of 2D/3D FRAP with given bleaching intensity profiles were in close agreement with those deduced from our measurement, we attempted to correct w_0 by analysis of fluorescence images recorded at $t = 0$ s immediately after photobleaching process. Following the method proposed by Pucadyil and Chattopadhyay,[12] we obtained w_0 (corrected) $= 18.0\,\mu$m which is approximately 14.7% smaller than w_0 measured by the beam profiler. This error could be partially caused by diffusion of the particles before the first image was acquired after photobleaching as there was an inevitable time lag due to limited frame rate of the camera used in our system. Applying the corrected w_0, D_{FRAP} values were recalculated and listed in Table 1. After correction, D_{FRAP} falls in the range 1.95–2.35 μm^2/s for 210 nm and 0.89–1.11 μm^2/s for 500 nm particles and those are reasonably in agreement with D_{SPT} and D_{SE} except for D_{FRAP} determined by Eq. (2).

As the light paths for illuminating the sample with the laser beam and the mercury lamp are separated in our *i*FRAP-SPT system, FRAP and SPT measurements can be applied simultaneously to a binary mixture. We used the fluorescent particles with large stokes shift (488 nm/560 nm). We captured the time series images through the objective. By separating the emission wavelength of the fluorescence, we could conduct FRAP and SPT analyses to determine D_{FRAP} of 70 kDa dextran and

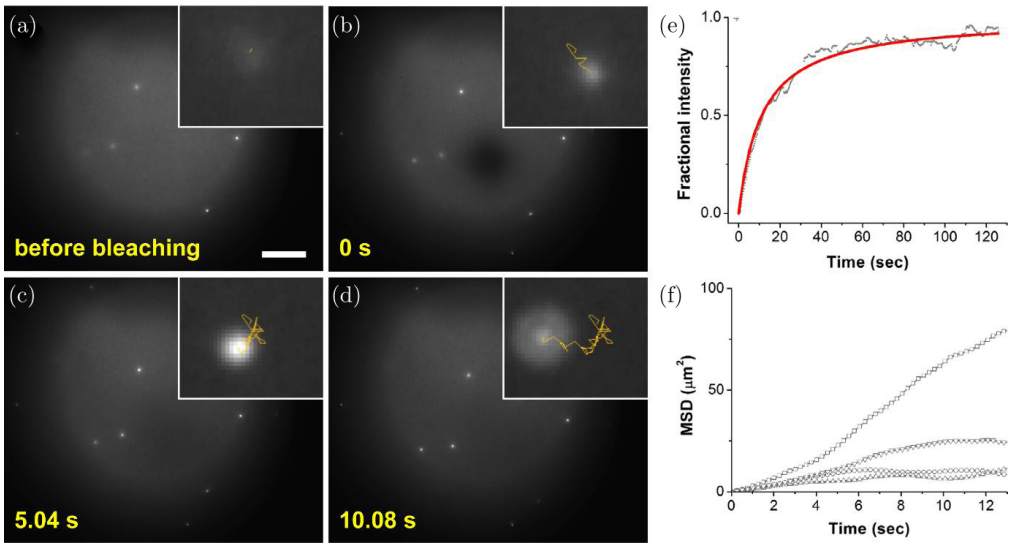

Fig. 4. FRAP and SPT images are acquired simultaneously through the *i*FRAP-SPT system in a single platform. (a) Before photobleaching. (b) $t = 0$ s. (c) $t = 5.04$ s. (d) $t = 10.08$ s. Insets present the particle trajectories obtained from SPT experiments. Scale bar = 50 μm. Diffusion coefficients of fluorescein dextran (70 kDa) and fluorescent particle (1 μm) are measured by (e) FRAP and (f) SPT, respectively.

D_{SPT} of 1 μm particle mixed in distilled water, respectively. Figures 4(a)–4(d) show the FRAP and the SPT images (insets) obtained by *i*FRAP-SPT platform. The half time recovery ($t_{1/2}$) calculated from the fluorescence recovery curve allows us to estimate the diffusion coefficient of the fluorescein dextran (Fig. 4(e)). The MSD-time plot for the random motion of each fluorescent particle also allows us to estimate the diffusion coefficient (Fig. 4(f)). There was a good agreement between $D_{\mathrm{SPT}} = 0.44 \pm 0.12\,\mu\mathrm{m}^2/\mathrm{s}$ ($n = 4$) (Fig. 3(c)) and $D_{\mathrm{SE}} = 0.48\,\mu\mathrm{m}^2/\mathrm{s}$ for 1 μm particle. D_{FRAP} of the 70 kDa dextran was $8.24 \pm 0.15\,\mu\mathrm{m}^2/\mathrm{s}$ and $7.42 \pm 0.12\,\mu\mathrm{m}^2/\mathrm{s}$ for the bleaching intensity with the 2D and 3D Gaussian profiles, respectively.

The hydrodynamic radius of the 70 kDa dextran was known to be 5.1 ± 0.7 nm[13] and empirical equation of the hydrodynamic radius of FITC-dextran was reported[14] as follows:

$$r_h = 0.015 M_w^{0.53\pm0.02}, \tag{8}$$

and the calculated hydrodynamic radius (r_h) is 5.6 ± 1.4 nm where M_w is the molecular weight (g/mol). The viscosities for the 70 kDa dextran at three different concentrations are given by a manufacturer.[15] The concentration of the solution of our fluorescein dextran sample was 20 mg/mL. From the extrapolation of the viscosity shown in Ref. 15, the viscosity was calculated to be 1.336 cP at the concentration of our dextran sample. Assuming that the shape of fluorescein dextran is spherical, $D_{\mathrm{SE}} = 14.31\,\mu\mathrm{m}^2/\mathrm{s}$ from the Stokes–Einstein equation. D_{FRAP} for 70 kDa dextran measured in aqueous solution by other research groups exhibits a wide range of values depending on experimental conditions including the concentration of dextran solution, the temperature of solution and method for FRAP measurement; $23\,\mu\mathrm{m}^2/\mathrm{s}$ for 4 mg/mL at 23°C,[16] $33\,\mu\mathrm{m}^2/\mathrm{s}$ for 25 mg/mL at 19°C,[17] and $43.7\,\mu\mathrm{m}^2/\mathrm{s}$ for 10 mg/mL at 22°C.[18] It is remarkable that the diffusion coefficient for the dextran sample was estimated to be in the same order of magnitude compared to that measured by the FRAP in spite of the assumptions of the shape and viscosity for the dextran used in this study. These results assure that the diffusion coefficient measured by our *i*FRAP-SPT is reasonably accurate.

For the FRAP technique, the diffusion coefficient is estimated by measuring the spot size, w, and the half time, $t_{1/2}$, as can be seen in the Eqs. (2)–(4). Then the combined uncertainty is associated with the uncertainty in the spot size and the uncertainty in the half time. The combined uncertainty is calculated from the following equation[19]:

$$U_{D\_\mathrm{FRAP}} = \sqrt{\left(\frac{\partial D}{\partial w} U_w\right)^2 + \left(\frac{\partial D}{\partial t_{1/2}} U_{t_{1/2}}\right)^2}, \tag{9}$$

where U indicates the uncertainty and the subscripts imply the measurement parameters.

The uncertainty in $D_{\mathrm{FRAP}} = 0.224w^2/t_{1/2}$ given by Soumpasis[2] can be calculated as follows:

$$U_{D\_\mathrm{FRAP}} = \sqrt{\left(0.448\frac{w}{t_{1/2}}U_w\right)^2 + \left(-0.224\frac{w^2}{t_{1/2}^2}U_{t_{1/2}}\right)^2}. \tag{10}$$

The beam spot size of this study was measured to be 12.6–24.5 μm and the half time was 10.48–44.68 s. As the uncertainties associated with the beam spot size and the half time are measured as 14.7% and 8.5%, respectively, we can evaluate the uncertainty propagation due to the beam spot size and the half time. The upper bound of uncertainty of the FRAP technique is calculated to be 18.6% approximately.

The uncertainty of the SPT technique can be estimated in a similar way to the case of FRAP as follows:

$$\begin{aligned} U_{D\_\mathrm{SPT}} &= \sqrt{\left(\frac{\partial D}{\partial \mathrm{MSD}}U_{\mathrm{MSD}}\right)^2 + \left(\frac{\partial D}{\partial \Delta t}U_{\Delta t}\right)^2} \\ &= \sqrt{\left(\frac{1}{4\Delta t}U_{\mathrm{MSD}}\right)^2 + \left(-\frac{\mathrm{MSD}}{4\Delta t^2}U_{\Delta t}\right)^2}. \end{aligned} \tag{11}$$

The uncertainties associated with a statistical error in MSD and time step are found to be 11% and 1%, respectively, thus we can show that the uncertainty propagation due to the MSD and the time step is calculated to be approximately 11.0%, which is less than the uncertainty propagation of the FRAP technique. The SPT technique shows better performance than the FRAP technique in the sense of the uncertainty. The uncertainty of the FRAP technique is mainly influenced by the measurement of bleaching spot size, which involves errors caused from the resolution and acquisition rate of the images. The uncertainty analysis implies that the performance of the FRAP can be improved by reducing the uncertainty in the measurement of bleaching spot size and the half time. The application of the technique relevant to the enhancing the image quality in the measurement will be a subject of the upcoming research.

5. Conclusion

By our novel image-based FRAP technique, we were able to narrow down the errors of diffusion coefficients originated from several artifacts. We demonstrated that our *i*FRAP-SPT system could measure diffusions of dense dextran macromolecules and sparse microparticles mixed in the same aqueous solution by FRAP and SPT, respectively, in single platform. The *i*FRAP-SPT system developed in this study may offer new opportunities to more accurately estimate the diffusion of biomolecules and has potential to be extended to the quantification of hindered diffusion or anomalous diffusion. Our *i*FRAP-SPT can be used for not only cellular membrane dynamics but also quantitative analysis of the spatiotemporal distribution of the solutes in small-scale analytical devices.

Conflicts of Interest

There are no conflicts of interest to declare.

Acknowledgments

This work was supported by grants from the National Research Foundation (NRF) (NRF-2019R1A2C2088973) funded by the Ministry of Education and the Korea Evaluation Institute of Industrial Technology (KEIT) (20011377) funded by the Ministry of Trade, Industry & Energy, Republic of Korea.

References

1. D. Axelrod, D. E. Koppel, J. Schlessinger, E. Elson, W. W. Webb, "Mobility measurement by analysis of fluorescence photobleaching recovery kinetics," *Biophys. J.* **16**, 1055–1069 (1976).
2. D. M. Soumpasis, "Theoretical analysis of fluorescence photobleaching recovery experiments," *Biophys. J.* **41**, 95–97 (1983).
3. T. J. Feder, I. Brust-Mascher, J. P. Slattery, B. Baird, W. W. Webb, "Constrained diffusion or immobile fraction on cell surfaces: A new interpretation," *Biophys. J.* **70**, 2767–2773 (1996).
4. K. Braeckmans, L. Peeters, N. N. Sanders, S. C. De Smedt, J. Demeester, "Three-dimensional fluorescence recovery after photobleaching with the confocal scanning laser microscope," *Biophys. J.* **85**, 2240–2252 (2003).
5. P. M. Haggie, J. K. Kim, A. S. Verkman, "Tracking of quantum dot-labeled CFTR shows near immobilization by C-Terminal PDZ interactions," *Mol. Biol. Cell.* **17**, 4937–4945 (2006).
6. K. Ritchie, X. Y. Shan, J. Kondo, K. Iwasawa, T. Fujiwara, A. Kusumi, "Detection of non-brownian

diffusion in the cell membrane in single molecule tracking," *Biophys. J.* **88**, 2266–2277 (2005).
7. M. J. Saxton, K. Jacobson, "Single-particle tracking: Applications to membrane dynamics," *Annu. Rev. Biophys. Biomol. Struct.* **26**, 373–399 (1997).
8. L. Guo, J. Y. Har, J. Sankaran, Y. Hong, B. Kannan, T. Wohland, "Molecular diffusion measurement in lipid bilayers over wide concentration ranges: A comparative study," *Chem. Phys. Chem.* **9**, 721–728 (2008).
9. M. Woringer, I. Izeddin, C. Favard, H. Berry, "Anomalous subdiffusion in living cells: Bridging the gap between experiments and realistic models through collaborative challenges," *Front. Phys.* **8**, 134 (2020).
10. E. B. Brown, E. S. Wu, W. Zipfel, W. W. Webb, "Measurement of molecular diffusion in solution by multiphoton fluorescence photobleaching recovery," *Biophys. J.* **77**, 2837–2849 (1999).
11. G. K. Batchelor, "The effect of Brownian motion on the bulk stress in a suspension of spherical particles," *J. Fluid Mech.* **83**, 97–117 (1977).
12. T. J. Pucadyil, A. Chattopadhyay, "Confocal fluorescence recovery after photobleaching of green fluorescent protein in solution," *J. Fluoresc.* **16**, 87–94 (2006).
13. J. J. Choi, S. Wang, Y. S. Tung, B. Morrison III, E. E. Konofagou, "Molecules of various pharmacologically-relevant sizes can cross the ultrasound-induced blood-brain barrier opening in vivo," *Ultrasound Med. Biol.* **36**, 58–67 (2010).
14. S. C. De Smedt, A. Lauwers, J. Demeester, "Structural information on hyaluronic acid solutions as studied by probe diffusion experiments," *Maromolecules*, **27**, 141–146 (1994).
15. Physical properties of dextran, http://www.dextran.net/dextran-physical-properties.html.
16. N. Periasamy, A. S. Verkman, "Analysis of fluorophore diffusion by continuous distributions of diffusion coefficients: Application to photobleaching measurements of multicomponent and anomalous diffusion," *Biophys. J.* **75**, 557–567 (1998).
17. J. V. C. Silva, P. D. S. Peixoto, S. Lortal, J. Floury, "Transport phenomena in a model cheese: The influence of the charge and shape of solutes on diffusion," *J. Dairy Sci.* **96**, 6186–6198 (2013).
18. J. Braga, J. M. Desterro, M. Carmo-Fonseca, "Intracellular macromolecular mobility measured by fluorescence recovery after photobleaching with confocal laser scanning microscopes," *Mol. Biol. Cell.* **15**, 4749–4760 (2004).
19. H. W. Coleman, W. G. Jr. Steele, *Experimentation and Uncertainty Analysis for Engineers*, John Wiley & Sons, New York (1989).